COMPUTATIONAL WING DESIGN STUDIES RELATING TO NATURAL LAMINAR FLOW

Edgar G. Waggoner
NASA Langley Research Center
Hampton, Virginia 23665

SUMMARY

Two research studies are described which directly relate to the application of natural laminar flow (NLF) technology to transonic transport-type wing planforms. Each involved using state-of-the-art computational methods to design three-dimensional wing contours which generate significant runs of favorable pressure gradients. The first study supported the Variable Sweep Transition Flight Experiment and involves design of a full-span glove which extends from the leading edge to the spoiler hinge line on the upper surface of an F-14 outer wing panel. Boundary-layer and static-pressure data will be measured on this design during the supporting wind-tunnel and flight tests. These data will then be analyzed and used to infer the relationship between cross-flow and Tollmien-Schlichting disturbances on laminar boundary-layer transition. A wing was designed computationally for a corporate transport aircraft in the second study. The resulting wing design generated favorable pressure gradients from the leading edge aft to the mid-chord on both upper and lower surfaces at the cruise design point. Detailed descriptions of the computational design approach are presented along with the various constraints imposed on each of the designs. Wing surface pressure distributions, which support the design objectives and were derived from transonic three-dimensional analysis codes, are also presented. Current status of each of the research studies is included in the summary.

INTRODUCTION

Computational fluid dynamics (CFD) is playing an increasingly important role in the aircraft design process. All major airframers are using CFD as a complement to wind-tunnel and flight testing. This can increase the efficiency of test facility utilization as well as significantly reduce the risks associated with a development program. Increases in computer speed and storage capabilities, in conjunction with developments in code solution algorithms and grid generation, have fostered development of powerful computer codes. Codes have been developed which can solve the complex transonic flow field around a multi-component aircraft configuration (refs. 1 and 2). In addition, these codes have proven to be robust and reliable, and they can be routinely relied upon in a preliminary design environment.

Two studies are described in this paper. The first is concerned with understanding the interaction of crossflow and Tollmien-Schlichting (TS) instabilities on laminar boundary-layer transition. The second study is an actual design of a natural laminar flow wing. Although each of these studies is concerned with various aspects of laminar flow, the theme of this discussion is the application of computational techniques in support of each of these programs.

Each study involved designing a wing or portion of a wing to generate a pressure distribution with certain characteristics. State-of-the-art computational techniques were used to accomplish the design tasks associated with each study. The designs will be experimentally verified through wind-tunnel testing at the NASA Langley Research Center.

A brief description of the various two- and three-dimensional computer codes is included in the following section. Subsequent sections describe each of the studies in some detail. Included are descriptions of study objectives and constraints which impacted the design. A rather detailed description of the design process is included, along with appropriate examples of results at key stages during the design. Current status of the

studies is discussed, and a summary of the salient observations made during the two studies is included in the conclusion.

COMPUTATIONAL METHODS USED IN THE STUDIES

Several computer codes have been used to analyze the various configuration models and designs which have been evaluated during the present studies. Three-dimensional analyses have utilized both a full potential code, which is coupled with a three-dimensional integral boundary-layer code (TAWFIVE) (ref. 1) and an extended small-disturbance analysis code (WBPPW) (ref. 2) which has been verified extensively at NASA Langley Research Center (refs. 3 and 4). Three-dimensional automated design capability was realized using a Lockheed Georgia modified version of the FLO-22 NM code (ref. 5). The code has McFadden's design algorithm (ref. 6) and a quasi-Newton's method optimization procedure as an integral part of the code. The NYU airfoil code (ref. 7) and the two-dimensional option in the WBPPW code were used to provide the two-dimensional analyses. High-lift characteristics of airfoil designs were predicted with a subsonic panel code which includes an integral boundary-layer calculation (ref. 8).

WBPPW Analysis Code

The Wing-Body-Pod-Pylon-Winglet code, developed by Charles Boppe of Grumman Aerospace Corporation, is characterized by a unique grid-embedding technique which provides excellent flow-field resolution about various configuration components. The code solves for the flow field about a wing-fuselage configuration which can include engine pods or stores, wing pylons, and wingtip-mounted winglets at transonic speeds. Using finite-difference approximations, a modified small-disturbance potential-flow equation is iteratively solved in a system of multiple embedded grids. The modifications to the classical small-disturbance equation are in the form of extra terms, which, when added to the equation, provide more accurate resolution of shock waves with large sweep angles and a better

approximation of the critical velocity where the full potential equation changes from elliptic to hyperbolic in type.

The computational space used in the method is filled with a relatively crude global grid system. This grid is stretched to planes corresponding to infinity in all directions. The global grid basically serves two purposes. It provides the proper representation of the effects of the configuration on the far-field and, conversely, the effects of the far-field conditions on the flow field near the configuration. In addition, the crude grid provides the channels of communication between the various embedded fine grids.

Fine grid regions around components of interest are embedded into the global continuous grid. The fine grids are distributed along the wing span and, if desired, may also encompass the fuselage, engine pods or stores, pylons, and/or a winglet. Within the fine grids, the resolution is much enhanced relative to the global grids. This allows far greater resolution in areas where flow-field gradients are large.

Viscous effects are approximated in the code by coupling a modified Bradshaw boundary-layer computation to the finite-difference potential-flow solution. The modified method provides a technique to extend a two-dimensional boundary-layer calculation to account for first-order sweep effects (ref. 9). The viscous effects are incorporated in the solution by adding the boundary-layer displacement slopes to the wing surface slopes. This modifies the wing surface to an equivalent "fluid" wing shape which is then analyzed by the potential flow code.

TAWFIVE Analysis Code

A computer code for the Transonic Analysis of a Wing and Fuselage with Interacted Viscous Effects (TAWFIVE) was also used in the study. The code utilizes the interaction of an inviscid and a viscous flow solver to obtain transonic flow-field solutions about wing-fuselage combinations. The outer inviscid flow field is solved using a conservative, finite-volume, full-potential method

based on FLO-30 by Caughey and Jameson. No modifications were made to the internal grid-generation algorithm in FLO-30, which is a body-fitted, sheared, parabolic coordinate system.

Viscous effects are computed using a compressible integral method which calculates three-dimensional boundary layers for wings. The code has the capability of computing laminar or turbulent boundary layers with the methods of Stock (ref. 10) and Smith (ref. 11), respectively. An important addition to the code is Streett's treatment of the wake (ref. 12). The wake model used in FLO-30 was replaced with a model which satisfies flow tangency on the wake displacement body and the pressure jump condition resulting from wake curvature. These changes in the code can make significant differences in results obtained on various configurations (ref. 12).

FLO-22NM Design and Analysis Code

The FLO-22NM (ref. 6) code is a wing alone transonic code which has the application of design and optimization algorithms included as solution options. The FLO-22 (ref. 13) solver has provided reliable nonconservative solutions to the full potential equation for a number of years. A design algorithm is included in the code based on the work of Bauer, Garabedian, and McFadden (ref. 6). By relating wing section contour changes to incremental changes in surface pressure distributions, a systematic procedure is established to modify a wing contour to achieve a desired target pressure distribution. Modifications to the original algorithm were made at Lockheed Georgia Company to extend the regions of the wing where the algorithm is applied. An option to employ a quasi-Newton's method optimization procedure (ref. 14) is available in the code. However, this option was not exercised during this study.

NYU Airfoil Code

The New York University airfoil analysis code written by Bauer, Garabedian, Korn, and Jameson (ref. 7) is used extensively by many researchers to provide two-dimensional viscous analyses of airfoils. The inviscid solution solves for the steady, isentropic, irrotational flow about an airfoil contour. Viscous corrections are provided by adding the turbulent displacement thickness to the airfoil surface. There is no laminar boundary layer calculated by the code. The momentum thickness is initialized at the transition point, which can be set arbitrarily. Using the turbulent boundary-layer method of Nash and Macdonald (ref. 15), the boundary-layer characteristics are computed using the results from the potential flow analysis and the airfoil geometric characteristics.

High-Lift Code

The high-lift code (ref. 8) developed at Lockheed Georgia Company and modified at NASA-Langley defines the subsonic viscid attached flow about two-dimensional multi-component airfoils. The viscous solution is obtained by interacting potential flow and a boundary-layer solution for the flow field. Potential flow approximations are made using a distributed vortex concept with the vortex singularity comprising the fundamental solution to the Laplace equation. Boundary-layer solutions employ representations of the laminar and turbulent boundary layer along with a transition model. Laminar boundary-layer separation criteria have also been included in the code and are used in the present study as an indication of low-speed maximum lift coefficients.

F-14 VARIABLE SWEEP TRANSITION FLIGHT EXPERIMENT

During the mid 1970's, NASA began the Aircraft Energy Efficiency (ACEE) program to develop fuel conservation technology for commercial transports (ref. 16). One aspect of the ACEE program that has received considerable research attention is the development of technology for viscous-drag reduction through natural laminar flow (NLF) and laminar flow control (LFC). Recent research at NASA has been encouraging relative to obtaining significant extents of laminar flow with either method or a combination of both.

An important question which must be answered in order to design wings which effectively utilize natural laminar flow relates to boundary-layer transition. It is known that for boundary layers in a three-dimensional flow environment there is an interaction between crossflow (CF) and TS instabilities that can cause transition to occur in an otherwise favorable environment (i.e., favorable pressure gradient, smooth surface, etc.) (ref. 17). In order to assist in identifying and quantifying the influence of the CF-TS interaction on wing boundary-layer transition, data are needed for various combinations of favorable pressure gradients, Reynolds numbers, and wing sweep angles.

To establish a data base for the transition data, NASA Langley and NASA Ames-Dryden have defined a variable sweep transition flight experiment (VSTFE) utilizing the F-14 aircraft. The objectives of this flight test are to obtain in-flight wing pressure and boundary-layer data which will be used to develop a reliable laminar boundary-layer transition prediction method. The approach to obtaining the flight data is to modify the F-14 wing outer panel by "gloving" on a foam and fiberglass panel contoured such that it generates favorable pressure gradients on the upper surface over a wide range of flight conditions (fig. 1). By using data obtained from analyses of the wing pressure distributions with a boundary-layer stability code and from flight-measured transition data, inferences will be made relative to the interaction of CF and TS instabilities on boundary-layer transition.

Extensive computations have been performed in support of the proposed flight-test program. These range from verification of the potential flow methods to the actual design of the contour for the outer panel glove. Many of the preliminary computations are reported in reference 18. One of the intents of this paper is to demonstrate how the computations have been utilized and relied upon during the glove design phase of the VSTFE. Initially pertinent questions were answered regarding the use of small-disturbance and full-potential transonic

analysis codes. Questions were addressed relative to geometric considerations resulting from the complexity of the F-14 aircraft (figs. 1 and 2), the applicability of two-dimensional codes to the design problem, and the ability of the three-dimensional codes to accurately predict the flow field on the configuration. Although these questions are discussed in reference 18, in the interest of completeness of the present discussion it seems appropriate to include a brief discussion of the code validation efforts which involved comparison of code prediction with flight test data.

Comparison of Computations and Flight-Test Data

Some wind-tunnel pressure data existed for the F-14; however, the data were sparse for the primary wing sweep angle (Λ_{LE} = 20°), the Mach number, and the lift range of interest in this study. In January 1984, a flight test was conducted on NASA's F-14A aircraft 1-X at the Dryden Flight Research Facility (ref. 19). The objective of the flight test was to explore the proposed flight envelope for the VSTFE and to obtain wing pressure data on the baseline aircraft. "Strip-A-Tubes" were bonded to the wing surface at four locations along the wing span. The pressure tubes were aligned with the free-stream flow when the wing leading edge was swept 19°. For this sweep angle, the tube spanwise positions corresponded to 40, 56, 73, and 87 percent of the semispan.

Wing pressure data were obtained over a wide range of Mach numbers, lift coefficients, altitudes, and wing sweeps. The ranges of the various parameters are summarized in the table below.

Table 1. - Flight-Test Conditions

Leading-edge sweep	20°-30°
Mach number	0.6-0.85
Altitude, ft	25K-35K
Lift coefficient	1-2g flight

From these data, four flight points were designated to be of primary interest. Three of these points correspond to corners of the

flight envelope for the VSTFE, and the remaining point was an intermediate flight condition. The four points are listed as follows:

Point	M	Altitude, ft	C_L
1	0.70	25,000	0.35
2	0.70	35,000	0.52
3	0.75	25,000	0.33
4	0.80	35,000	0.39

Points 1 and 2 correspond to the minimum and maximum altitudes where data will be obtained for level flight at M = 0.7, while point 4 corresponds to the maximum altitude level flight at M = 0.80. All of these data are for a wing sweep angle of 19°. Although data were obtained at sweep angles to 35°, the 'Strip-A-Tubes' were not aligned with the free-stream flow at the higher sweep angles. This misalignment could easily have compromised the corresponding data, since the tubes are raised off the wing surface.

These data were used to compare predictions from the TAWFIVE and WBPPW codes. The computational models for each of these codes included a wing and fuselage; however, the models did not include either horizontal or vertical tails. Therefore, in order to circumvent the problem of matching the total lift coefficient, all analyses were performed at the flight Mach number and measured angle of attack. The WBPPW code was run for 100 crude and 200 crude/fine iterations. Transition was specified at 5-percent of the chord on the upper and lower surfaces. The 2-D strip boundary-layer solution was interacted with the inviscid solution every 20 iterations. The TAWFIVE code was run for 100 crude, 100 medium, and 200 fine-mesh iterations. Transition was specified at the leading edge on both surfaces. Viscous effects were incorporated into the solution by calculating the full 3-D boundary layer three times (at iterations 100, 150, and 200) on the finest mesh. Solution residuals obtained were of the order of 10^{-4}.

The comparisons between the computations and the flight-test data are presented to discern the types of correlation possible between the experimental and computational data obtained in an engineering environment rather than to judge which code is 'best' or 'worst.' Two important points need to be reiterated in this regard:

1. The codes were not run to ultimate convergence, rather, they were converged to engineering accuracy.

2. No attempt was made to match lift coefficient, leading-edge pressure expansion, etc. Solutions were obtained at the flight Mach number, angle of attack, and altitude.

Overall, the comparisons presented in figures 3 to 6 are quite good. Before addressing specific points observed in the comparisons, several broad observations are appropriate. There are indications that the leading-edge slat is deflecting under flight load conditions. Evidence of this is apparent to some degree in each of the figures. Notice the pressure distributions over the forward 10 percent of the chord on the upper surface. The characteristic of the flow expansion at the leading edge followed by a compression is suspicious, particularly, since neither code predicts this type of characteristic. Evidence to support this hypothesis was obtained when static loadings corresponding to the flight loads were applied to the wing. By measuring surface deflections, it was obvious the slat was deflecting relative to the main wing structure.

The other observation concerns differences in the code predictions. Where differences in leading-edge expansion are observed (i.e., fig. 4), the full-potential code predicts more expansion at the leading edge than the small-disturbance code. This is consistent with the code formulation. Two points should be mentioned concerning shock waves (figs. 5 and 6). The grid in the WBPPW code has approximately three times higher resolution near the shock location than the TAWFIVE code (0.01x/c vs. 0.03x/c). This accounts for the 'sharper' shock resolution observed in the WBPPW results. In addition,

the shock is located forward in the WBPPW code relative to the TAWFIVE code. This difference can be traced to the basic differencing scheme formulations employed in the code. The WBPPW code uses nonconservative differencing, while the TAWFIVE code uses a conservative differencing scheme. The most obvious effect of this difference is the location of shock waves. Nonconservative differencing tends to affect the solution in the same manner as viscous effects so that shock waves tend to be predicted further forward.

The data for level flight at M = 0.7 and 25,000 feet are presented in figure 3. The comparisons between these data and experiment are excellent at both span locations presented. The loading at the outboard span location is slightly overpredicted by each of the analysis codes.

The high altitude (35,000 feet) , M = 0.70 data are presented in figure 4. This case shows the maximum effect of leading-edge slat deflection on the pressure distributions. Note also that the maximum difference in the computational predictions at the leading edge is observed here. Aft of 20-percent chord, the comparisons are excellent on the upper surface. However, the predictions of lower surface pressure distributions are significantly different from the experiment at the inboard station. The mechanism driving these differences is not fully understood at this time.

Quite good comparisons of computations and experiment are obtained for the intermediate (M = 0.75) case presented in figure 5. Evidence of the differences in shock prediction is observed at the inboard span location. However, the data for the high altitude (35,000 feet), high Mach (M = 0.80) case present a more graphic example of the code differences in figure 6. Note the agreement between the codes and the data over the forward part of the upper surface ahead of the shock. The shock predicted from the TAWFIVE code is approximately 5-percent chord aft and smeared relative to the shock predicted by the WBPPW code. This is consistent with the previous discussion.

Overall, the agreement between the flight-test data and the computational predictions from each code is excellent. All the differences observed between the computational results and between the computational results and experiment can be accounted for, except those shown in figure 4 for the pressure distributions on the rear part of the lower surface. These particular differences will not impact the way the codes will be applied in the design procedures.

Glove Design Constraints

Before a detailed description of the design steps and the supporting data are presented, the physical constraints of the actual modification should be addressed. These constraints had a significant impact on the design process. Although the constraints changed often over the course of the design study, only the final constraints and supporting rationale will be presented herein.

The wing upper surface was allowed to be modified from the leading edge aft to approximately the 60-percent chord line. Modifications to the lower surface were limited to the first 10 percent of the chord. The upper surface constraint was imposed to stop the glove modification in front of the spoiler hinge line, since the spoilers are used for roll control over a portion of the flight envelope. Consideration of the techniques employed in manufacturing the glove was responsible for the lower surface constraint being imposed.

Instrumentation leads were to be routed inside the leading edge of the glove, hence it was necessary to extend the glove leading edge 2 inches in front of the actual leading edge of the wing. There was also concern over slat movement under flight-loading conditions. This could have possibly caused undesirable contour changes in the glove shape. To minimize this possibility, the glove thickness was constrained to be a minimum of 0.65 inches over the upper surface. Under static loading conditions this thickness of foam and fiberglass was suffi-

cient to absorb any relative movement of the slot and the main wing element. This minimum thickness constraint in turn posed another constraint. In order to maintain adequate spoiler effectiveness, the thickness of the glove at the spoiler hinge line was limited to a maximum of 1 inch.

It is obvious that these are quite stringent constraints from a design standpoint. Detailed descriptions of the design steps and supporting data are included in the following discussion.

Glove Design Procedures

Based on the trends which were observed in the wing pressure data and the excellent comparisons which were obtained with the potential flow analysis codes, it was felt that an integrated two-dimensional/three-dimensional analysis and design process could be effectively formulated. The procedure, which evolved during the design effort, was not formulated a priori but did follow this loosely defined integrated approach.

The design point was chosen which corresponded to a "worst case" condition for the targeted Mach number of interest (M = 0.70). Because of the difficulty of maintaining favorable pressure gradients near the wing leading edge, the angle of attack for 1-g flight at the highest altitude in the test envelope was designated the design point. If a slightly favorable pressure gradient could be generated from the leading edge to the pressure rise at that condition, then reducing the altitude, hence the total lift coefficient and angle of attack required for level flight, would yield a more favorable pressure gradient. The design point corresponded to 1-g flight at M = 0.70 and 35,000 feet.

Five defining stations were chosen to be recontoured with linear lofting utilized between the defining stations. These corresponded to the inboard and outboard extent of the gloved region, where laminar flow was desired, and three intermediate defining stations. By relying on two-dimensional analyses, simple sweep corrections, and design procedures which generate

modifications to pressure distributions within specified physical constraints, upper surface contours were defined for each defining station which met the aerodynamic and physical constraints. The design procedure employed was a relatively simple algorithm which relates changes in local surface curvature to increments in surface pressure coefficients. The resulting curvature changes could be integrated to yield surface ordinate increments while monitoring the various physical constraints on the glove contour. Pressure distributions for a range of lift coefficients for the mid-span defining station are presented in figure 7. A sectional lift coefficient of 0.60 corresponds to the "worst case," and the other values to less severe cases. Note the favorable pressure gradient aft to the pressure rise for the range of lift coefficients presented.

After two-dimensional designs were completed for the five defining stations, the question of three-dimensional effects was addressed. The recontoured outer panel was modeled and analyzed in a three-dimensional analysis and design code (ref. 5). This allowed the identification of adverse three-dimensional effects resulting from the wing planform, twist distribution, etc. Two adverse characteristics were observed in the three-dimensional pressure distribution (fig. 8) which were not evident in the two-dimensional analyses. This includes a pressure peak at the wing leading edge and a flow expansion just forward of the shock. Of course, it was desirable to remove the adverse pressure gradient associated with the leading-edge pressure peak and to minimize the flow acceleration just forward of the shock. As described previously, the code has a design option available. A target pressure distribution was defined at each of the defining stations to minimize the adverse effects (fig. 8). The design option in the code was then employed to modify the wing outer panel to minimize the difference between the predicted and target pressure distributions. This step in the design process yielded modified contours for each of the defining stations.

These five new defining station airfoils were examined relative to the smoothness of their curvature distributions and constraint violations. Where appropriate, refairing and smoothing of the new contours were employed. This yielded final smoothed contours which met the design constraints at each of the defining stations. A typical contour is presented in figure 9 showing its relationship to the F-14 baseline contour at that wing station. Two-dimensional analyses were used to verify that no adverse effects had inadvertently shown up in the pressure distributions (fig. 10).

However, final computational verification of the design was realized by analyzing the entire configuration (fuselage, nacelles, strake, and outer panel) in the TAWFIVE code. Results presented in figure 11 show that the design objectives were realized over the range of lift coefficients corresponding to the altitudes of interest at $M = 0.7$. Data are also presented for a glove designed by Boeing for a design Mach number of 0.8. This glove will be flown concurrently with the NASA-designed glove. Data are presented for the $M = 0.7$ and $M = 0.8$ flight conditions. The boundary-layer analysis for the high altitude case at $M = 0.8$ (fig. 11(c)), gave no evidence of flow separation. Since the computational analysis predicted acceptable results and the design constraints were met, the glove design was frozen at this point.

VSTFE Status

Glove design has been completed for the VSTFE, and fabrication is underway for a wind-tunnel test to be conducted in the NTF during the early summer of 1985. The objectives of the test are to obtain data to verify the glove design and safety-of-flight data for support of the flight test program. Flight test instrumentation techniques will be validated in a program which will be flown in the late summer or early fall of 1985. A 'clean-up' glove has been fabricated for the F-14 outer panel which employs the physical constraints described previously and corresponds to the baseline F-14 outer panel contour. Any manufacturing or instrumentation problems uncovered during this program can be addressed before the NLF glove

experiment is flown. Manufacture of the NLF glove will commence in the last quarter of 1985 with the flight test following 9 to 12 months later.

HIGH ASPECT RATIO NLF WING

NASA has been interested in extending the applicability of the concept of natural laminar flow into the transonic speed regime, in addition to low- and medium-speed applications (ref. 16). In support of this objective, a program was undertaken to incorporate the concept of NLF into a high aspect ratio, low sweep wing designed for a corporate transport configuration. Much of the design work had been accomplished prior to NASA's involvement in the program including identification of the configuration characteristics such as fuselage geometry and wing planform (fig. 12). However, the wing section contour had not been defined, and this provided the basis for this discussion. An objective was identified to design a wing contour which would generate a significant extent of laminar flow on both the upper and lower surfaces at a transonic cruise design point. In addition, there were aerodynamic and geometric constraints imposed on the design. In order to provide adequate volume for fuel and for landing gear storage, the wing was required to have a minimum thickness to chord ratio of 12.5 percent. The configuration was powered by a single engine which dictated a rather low landing speed requirement. To meet this requirement, a large wing area had been specified along with airfoils which had a maximum sectional lift coefficient of 3.8. The large wing area translated to a cruise design point at $M = 0.7$ at a wing lift coefficient of 0.25. A self-imposed constraint was that the design offer acceptable aerodynamic characteristics with a fully turbulent boundary layer on the wing (as opposed to the long runs of laminar flow) over the flight envelope.

Computational Design

Again an integrated two- and three-dimensional computational design approach was identified. Both two-dimensional and three-dimensional analysis codes which had

been verified for transport application were identified to be used. This includes the two-dimensional Garabedian and Korn (ref. 7) and high-lift codes (ref. 8). Three-dimensional analyses were provided by the small-disturbance WBPPW code (ref. 2) and the full-potential TAWFIVE code (ref. 1).

As previously discussed, the wing planform had been specified as having a wing area of 250 ft^2, an aspect ratio of 8.0, and a taper ratio of 0.35. The quarter-chord of the wing had essentially no sweep, which minimized crossflow influences on the laminar boundary layer. In addition, except for interactions in the wing-body juncture regions and near the wing tip, the flow field was essentially two-dimensional. This allowed much of the contour modification work to be accomplished two dimensionally, employing three-dimensional analyses to verify the configuration characteristics.

The initial airfoil design was a derivative of a medium-speed NLF airfoil design by Viken (ref. 20). This airfoil had been designed for a lift coefficient of 0.4, M = 0.4, and a Reynolds number of 10 million. At the design condition, the airfoil generated favorable pressure gradients back to approximately 70 percent of the chord on the upper and lower surfaces. Viken's medium-speed design was scaled down for the higher speed applications, and the trailing edge was modified to account for the lower design lift coefficient. Analysis of the resulting airfoil is included in figure 13 for M = 0.70 and a sectional lift coefficient of 0.25. Two features of the flow over the airfoil at these conditions caused concern. The slight pressure peak at the lower surface leading edge was not desirable from a laminar flow standpoint. Of greater concern, however, was the pressure gradient through the pressure rise (at approximately 70 percent of the chord). Computational analyses predicted boundary-layer separation at these conditions. At overspeed conditions, the boundary-layer separation would be worse.

A computational 'cut and try' approach was employed to modify the initial airfoil contour. Using two-dimensional analysis as a

guide, the mid-chord region of the upper and lower surfaces and the leading edge of the lower surface were modified to eliminate the undesirable flow characteristics at the design condition. Two-dimensional analysis of the final airfoil design is presented in figure 14 along with the pressure distribution from the initial design. Note the softening of the gradients through the pressure rise and the modification of the lower surface leading-edge pressure expansion. It is also important to note that the extent of favorable pressure gradient has been reduced to approximately 50 percent of the chord on the upper surface and 60 percent of the chord on the lower surface. Analysis indicated no evidence of flow separation at the design condition.

The two-dimensional analysis calculates a turbulent boundary-layer skin-friction drag coefficient as part of the viscous solution. Estimates of skin-friction drag reduction can be inferred from figure 15 based on an analysis at two Mach numbers over a range of sectional lift coefficients. Transition was fixed at 10 percent of the chord for both surfaces for the forward transition case and 50 to 65 percent of the chord on the upper and lower surfaces for the aft transition case. These show a reduction of turbulent skin-friction drag ranging from 50 to 70 percent. Note that there is no estimate of the contribution from the laminar boundary layer. In addition, the reader should use the absolute levels judiciously; however, the relative differences are representative.

Up to this point, the discussion has centered around two-dimensional design and analysis. Three-dimensional analyses were employed at appropriate checkpoints in the design process to monitor the possible generation of adverse three-dimensional effects. An example of the three-dimensional analysis is included in figure 16. The data presented show the effect of varying the boundary-layer transition location on the pressure distribution on the inboard portion of the wing span. As expected, these data show little change in the pressure distribution; however, more important is the fact that no boundary-layer separation is predicted with the forward transition location. These same

characteristics were evident at higher free-stream Mach numbers for cruise conditions.

Computational Wing Design Effort

Only a small amount of data directly concerned with the wing section design has been included in this paper. However, several areas were addressed during this study which are not described in detail or supported with data presentations herein. It seems appropriate to describe the complete wing design effort so that the reader can obtain an appreciation for the various design areas deemed important.

While the initial two-dimensional design effort was underway, three-dimensional analyses yielded initial spanwise loading distributions. This led to a rather involved study to define an appropriate twist distribution for the wing. Tradeoffs were made among various twist and airfoil section distributions along the span. Final decision will have to be made by factoring in economic and manufacturing considerations. During the study, an evaluation was made on a proposed planform modification. Analyses yielded the effect of the modification on design decisions which had already been made.

As the airfoil modifications were completed, they were analyzed as part of the complete configuration in the three-dimensional codes. Although the majority of the analyses were near the design point, off-design analyses were performed and monitored to ensure that design goals were being met. Of primary importance for the off-design case was the shock strength associated with the overspeed flight conditions.

In anticipation of improvements in the configuration stall characteristics, two drooped leading-edge extensions were designed. Outboard leading-edge extensions have been found to improve stability levels in the vicinity of stall for certain classes of general aviation aircraft. The two extensions designed corresponded to 2- and 3-percent chord extensions and were employed in the outboard 25 percent of the wing semi-span. Transonic and low-speed analysis codes were used to analyze these modifications.

Final Design Characteristics

The wing designed through the use of computational procedures yielded excellent aerodynamic characteristics. At the cruise design point, favorable pressure gradients were generated on the upper and lower surfaces to 50 and 60 percent of the chord, respectively. This should yield significant runs of laminar flow and reductions in viscous drag. In addition, there was no indication of boundary-layer separation when transition was specified at the wing leading edge. The wing possessed good aerodynamic characteristics from low-speed conditions up to $M = 0.80$. Analyses indicated a drag divergence Mach number of 0.75 at cruise. A trade-off between the aerodynamic and propulsion characteristics might yield a cruise Mach number slightly higher than 0.70. Through the use of airfoil modification techniques, the drooped leading-edge extensions were smoothly incorporated into the airfoil contours. Overall, the computational analyses indicated the wing achieved or exceeded the originally specified performance goals.

SUMMARY AND CONCLUSIONS

State-of-the-art potential flow analysis techniques have been relied on to support two design studies involving natural laminar flow. Two- and three-dimensional small-disturbance and full-potential equation analysis codes have been verified for application to the present studies by comparison with experimental data. The various codes were used in analysis and design modes to meet the design objectives and constraints. A process evolved during the studies which effectively integrated the two- and three-dimensional codes. Results proved the potential flow codes to be accurate and reliable, and provided significant confidence in the design to be investigated.

During the course of this preliminary study, several salient observations were made concerning the computer codes exercised. These are summarized below:

76

1. TAWFIVE and WBPPW analyses each provided excellent prediction of flight-test results when compared at flight angle of attack, Mach number, and Reynolds number for the F-14 aircraft.

2. The integrated two- and three-dimensional design process proved to be efficient. Detailed contour modifications were made utilizing two-dimensional codes. Adverse three-dimensional effects were identified and appropriate contour modifications incorporated using three-dimensional design and analysis codes.

3. The automated three-dimensional design code was reliable. However, when contour changes were required near shock locations, additional fairing and smoothing were required.

In conclusion, computational wing design methodologies were successfully applied in two unique programs. The two- and three-dimensional aerodynamic codes used in these studies proved to be robust and reliable in a stringent schedule environment. The automated design procedure yielded excellent results, and the inclusion of that procedure or a similar one in the three-dimensional analysis codes is being pursued. Some deficiencies in the capabilities of the codes were identified, and possible corrections and improved running strategies are being addressed. The final accuracy of the design methods will be evaluated when wind-tunnel tests of both configurations are completed.

REFERENCES

1. Melson, N. D.; and Streett, C. L.: TAWFIVE: A User's Guide. NASA TM-84619, September 1983.

2. Boppe, C. W.; and Stern, M.: Simulated Transonic Flows for Aircraft With Nacelles, Pylons, and Winglets. AIAA Paper 80-130, January 1980.

3. Waggoner, E. G.: Computational Transonic Analysis for a Supercritical Transport Wing-Body Configuration. AIAA Paper 80-0129, January 1980.

4. Waggoner, E. G.: Computational Transonic Analysis for an Advanced Transport Configuration with Engine Nacelles. AIAA Paper 83-1851, July 1983.

5. Raj, P.; and Reaser, J. S.: An Improved Full-Potential Finite-Difference Transonic-Flow Code (FLO22.5) for Wing Analysis and Design. Lockeed California Company Report 29759, November 1981.

6. Bauer, F.; Garabedian, P.; and McFadden, G.: The NYU Inverse Swept Wing Code. NASA CR-3662, January 1983.

7. Bauer, F.; et al.: Supercritical Wing Sections II. Lecture Notes in Economics and Mathematical Systems, vol. 108, Springer-Verlag, 1975.

8. Stevens, W. A.; Goradia, S. M.; and Braden, J. A.: Mathematical Model for Two-Dimensional Multi-Component Airfoils in Viscous Flow. NASA CR-1843, July 1971.

9. Mason, W. H.; et al.: An Automated Procedure for Computing the Three-Dimensional Transonic Flow Over Wing-Body Combinations, Including Viscous Effects. Air Force Flight Dynamics Laboratory Report AFFDL-TR-122, vol. I, October 1977.

10. Stock, W. H.: Integral Method for the Calculation of Three-Dimensional Laminar and Turbulent Boundary Layers. NASA TM 75320, 1978.

11. Smith, P. D.: An Integral Prediction Method for Three-Dimensional Compressible Turbulent Boundary Layers. RAE R&M 3739, 1974.

12. Streett, C. L.: Viscous-Inviscid Interaction for Transonic Wing-Body Configurations Including Wake Effects. AIAA Paper 81-1266, July 1981.

13. Jameson, A.; and Caughey, D. A.: Numerical Calculation of the Transonic Flow Past a Swept Wing. COO-3077-140, ERDA Math and Computer Laboratory, New York University, June 1977.

14. Kennelly, R. A.: Improved Method for Transonic Airfoil Design by Optimization. AIAA 83-1844, July 1983.

15. Nash, J. B.; and Macdonald, A. G. J.: The Calculation of Momentum Thickness in a Turbulent Boundary Layer at Mach Numbers up to Unity. Aeronautical Research Council C.P. No. 963, London, 1967.

16. James, R. L.; and Maddalon, D. V.: The Drive for Aircraft Energy Efficiency. Aerospace America, vol. 22, no. 2, February 1984, p. 54.

17. Hanks, G. W.; et al.: F-111 Natural Laminar Flow Glove Flight Test Data Analysis and Boundary Layer Stability Analysis. NASA CR-166051, January 1984.

18. Waggoner, E. G., et al.: Potential Flow Calculations and Preliminary Wing Design in Support of an NLF Variable Sweep Transition Flight Experiment. AIAA Paper 85-0426, January 1985.

19. Moes, T. R.; and Myer, R. R.: In-Flight Wing Pressure Distributions for the F-14A. NASA TM 85921, June 1985.

20. Viken, J. K.: Aerodynamic Design Considerations and Theoretical Results for a High Reynolds Number Natural Laminar Flow Airfoil. M.S. Thesis, George Washington University, January 1983.
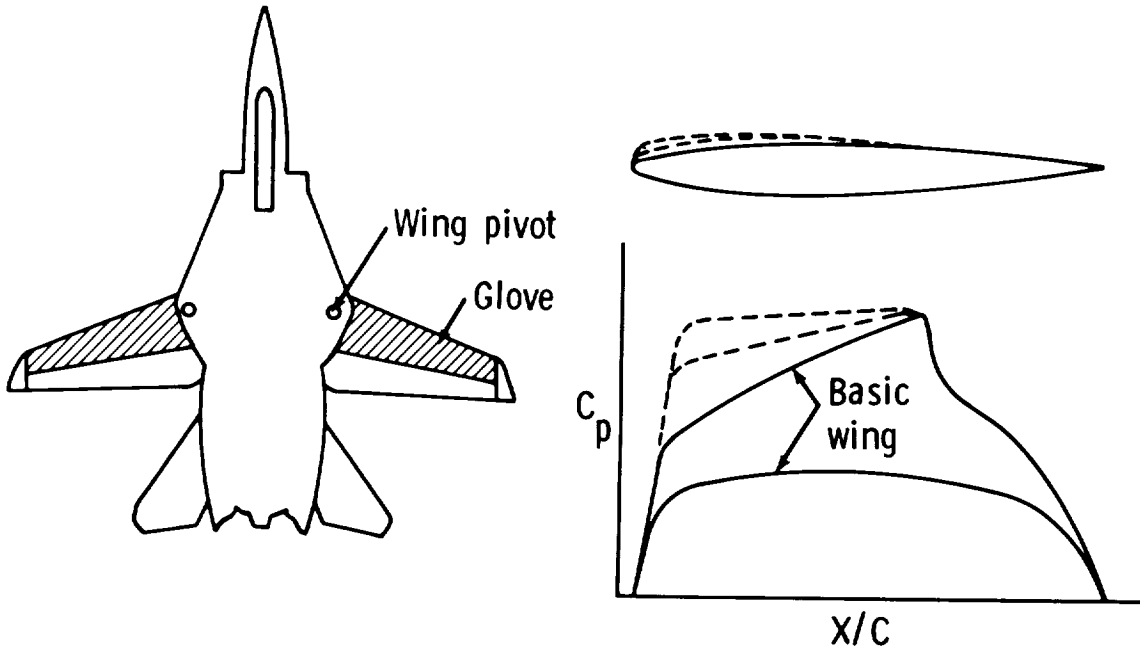
Figure 1.- F-14 planform and wing glove region.

SIDE VIEW   FRONT VIEW

Figure 2.- F-14 variable-sweep aircraft configuration.

79

$\eta=0.57$ $\eta=0.87$

⊙ Experiment
--- WBPPW
— TAWFIVE

C_p

$C_l=0.60$
0.40
0.20

Span station 200
M=0.70 Rn=20.0 million

C_p

Figure 7.- Two-dimensional analysis of design airfoil meeting final constraints.

M=0.70   α=3.6° C_L=0.62

mid-span

○ Analysis
---- Target pressure

C_p

Figure 1.- F-14 planform and wing glove region.

SIDE VIEW   FRONT VIEW
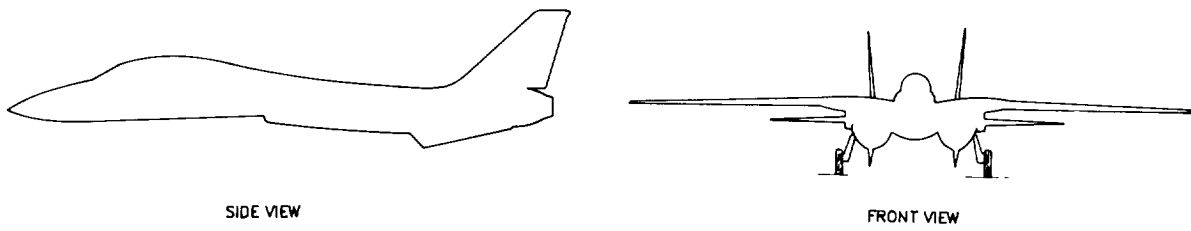
Figure 2.- F-14 variable-sweep aircraft configuration.

Figure 3.- Comparison of computational results and flight test data at an altitude of 25,000 ft for M = 0.70 and α = 2.1°.
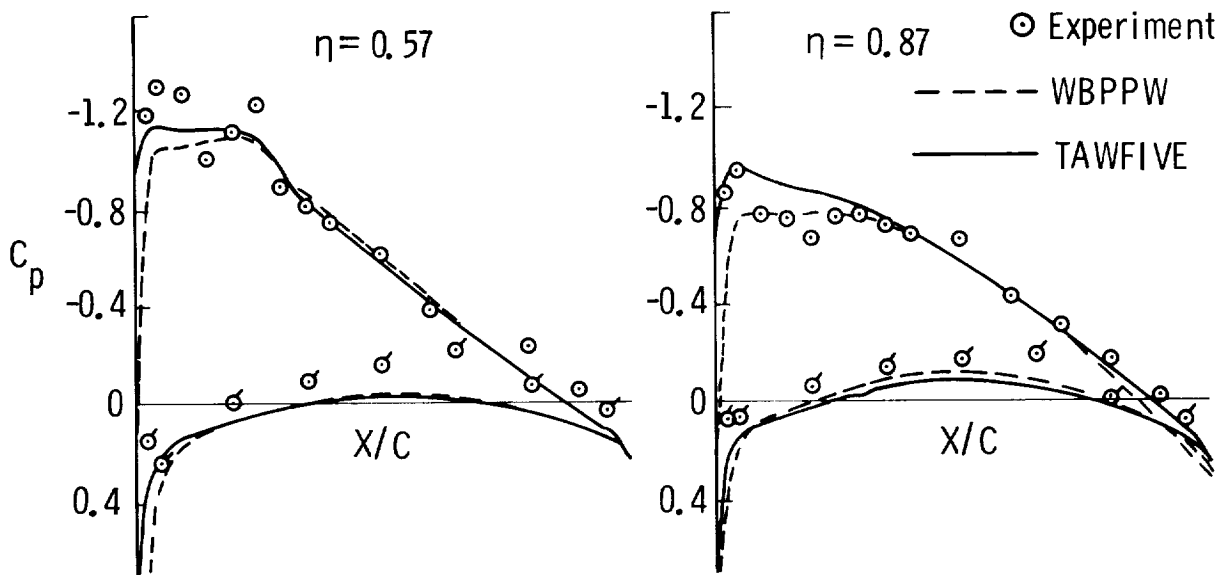
Figure 4.- Comparison of computational results and flight test data at an altitude of 35,000 ft for M = 0.70 and α = 3.6°.

80
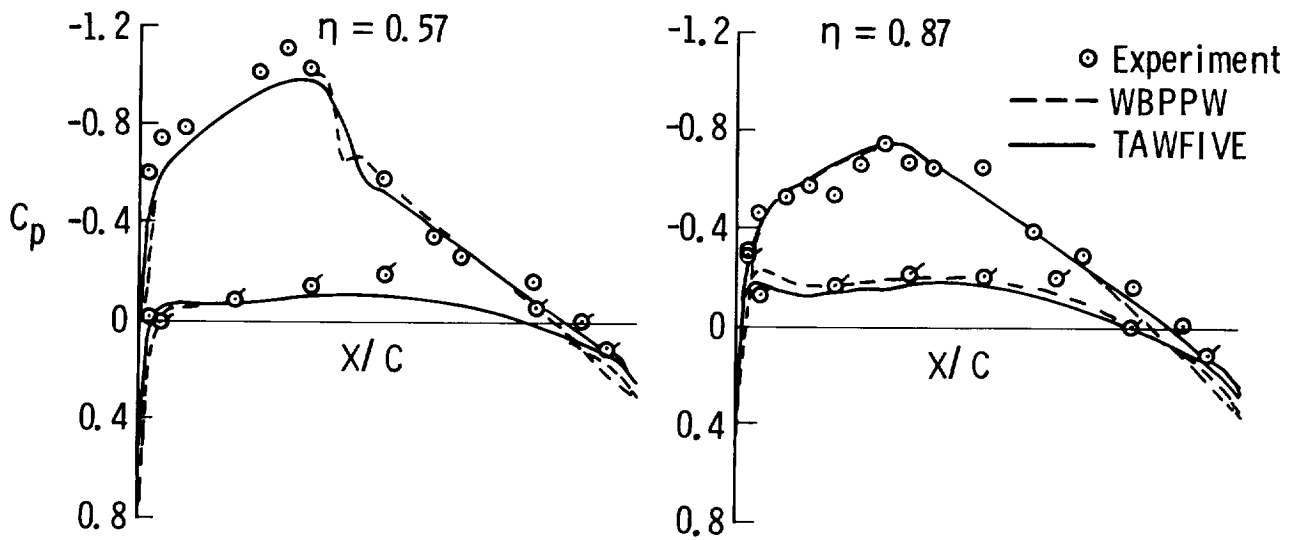
Figure 5.- Comparison of computational results and flight test data at an altitude of 25,000 ft for M = 0.75 and α = 1.7°.
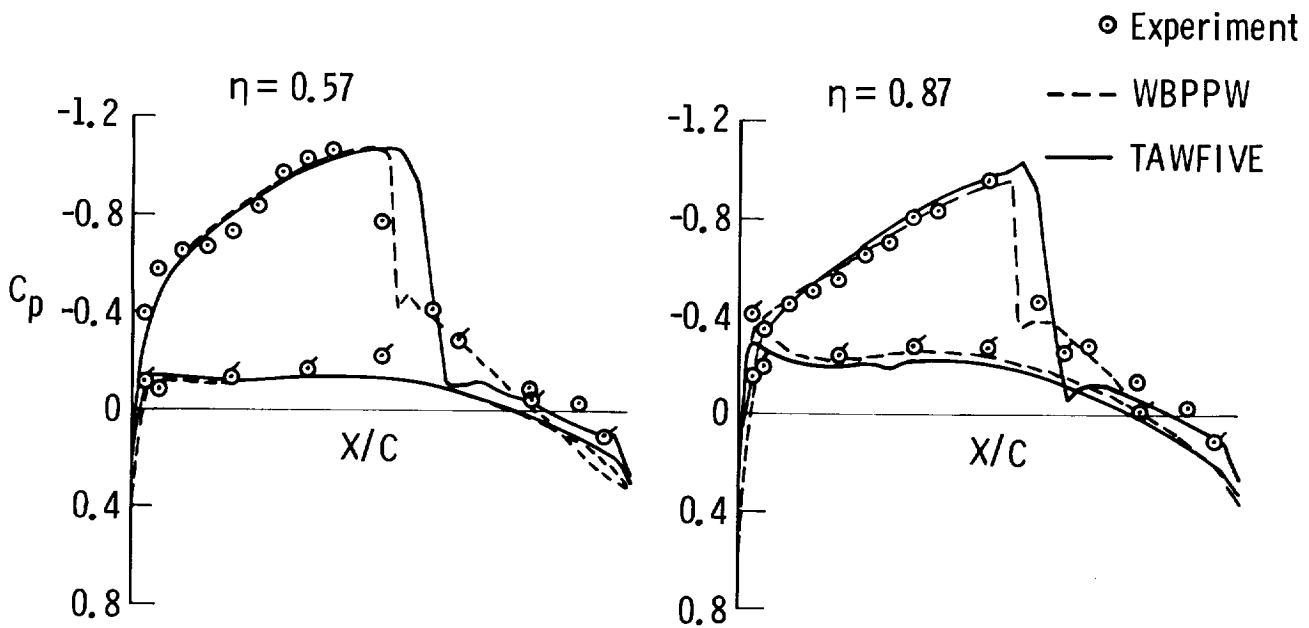
Figure 6.- Comparison of computational results and flight test data at an altitude of 35,000 ft for M = 0.80 and α = 1.4°.
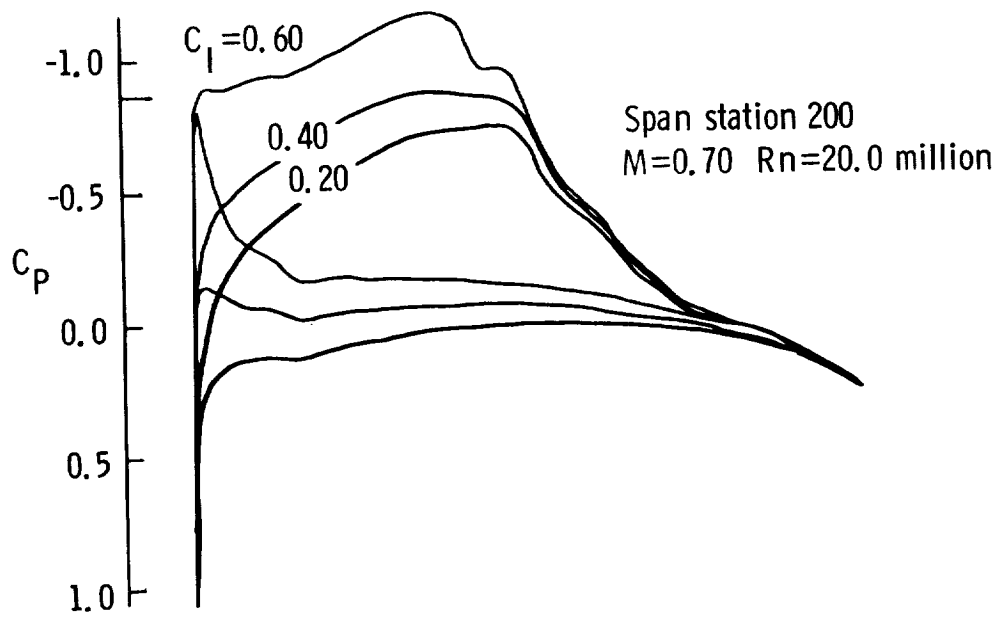
Figure 7.- Two-dimensional analysis of design airfoil meeting final constraints.
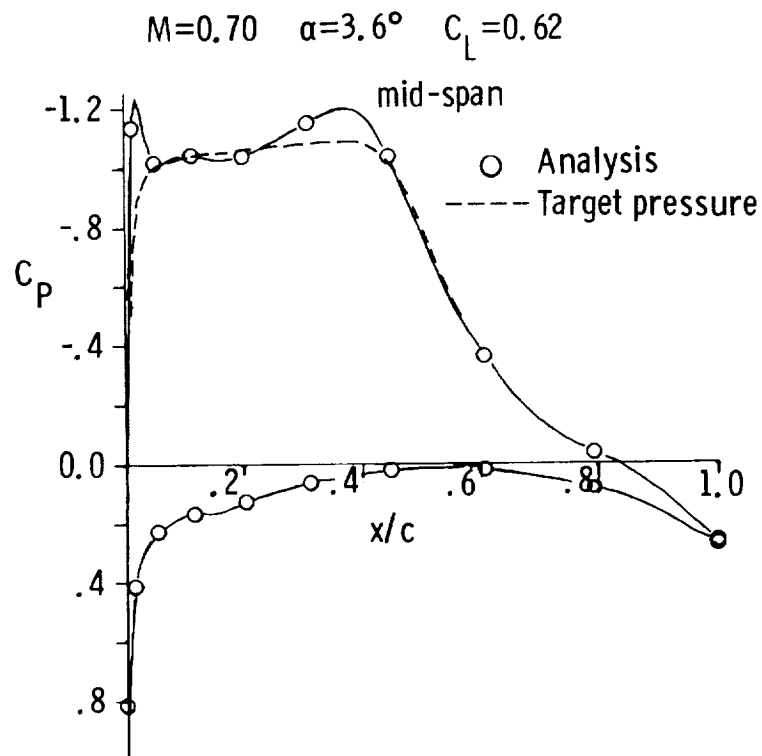
Figure 8.- Three-dimensional analysis and target pressures.

Span Station 200

--- Gloved airfoil
—— Baseline F-14 airfoil
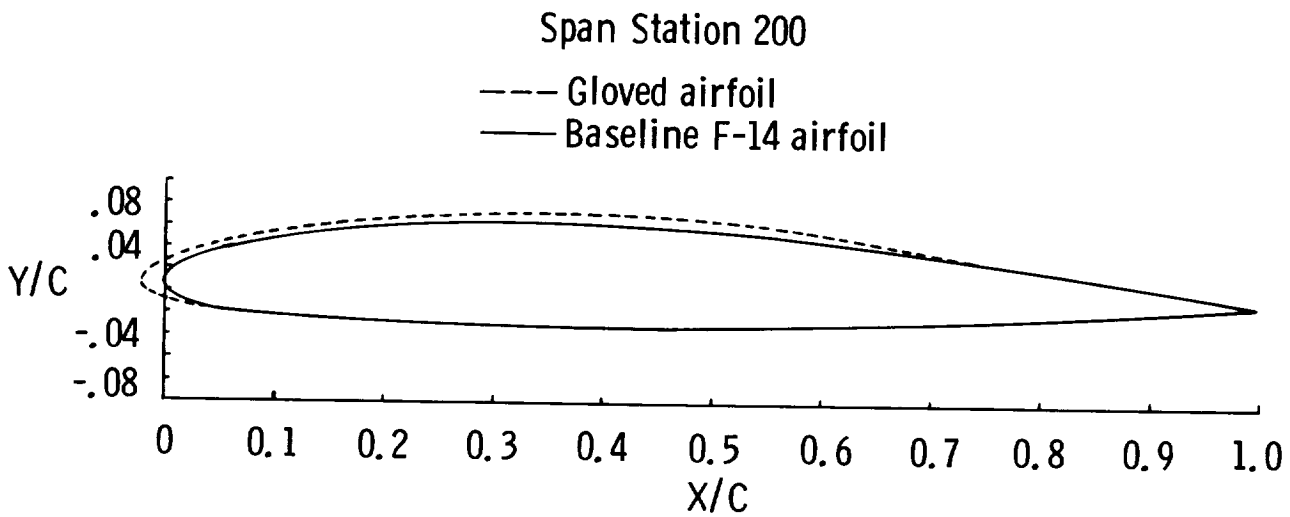
Figure 9.- Baseline F-14 section and glove design.

Span station 200
M=0.70 Rn=20.0 million

C_l=0.60
0.40
0.20
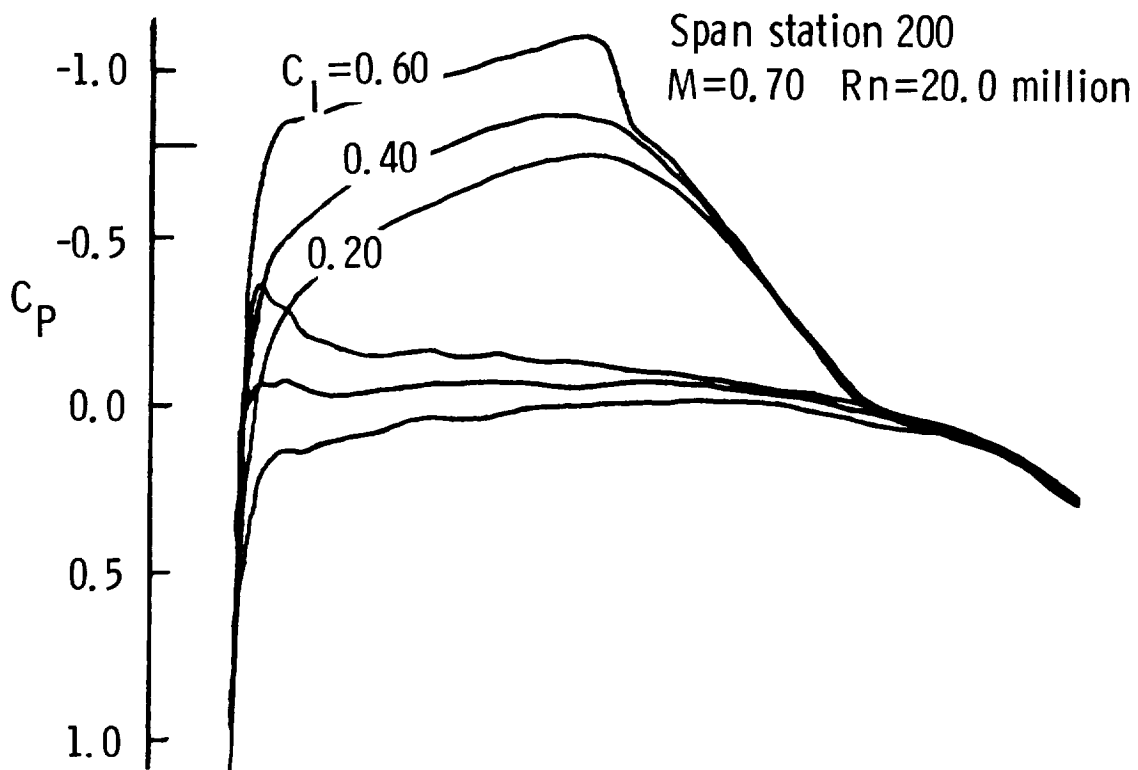
Figure 10.- Two-dimensional analysis of final F-14 glove design.

(a) M = 0.7; α = 0.7°.
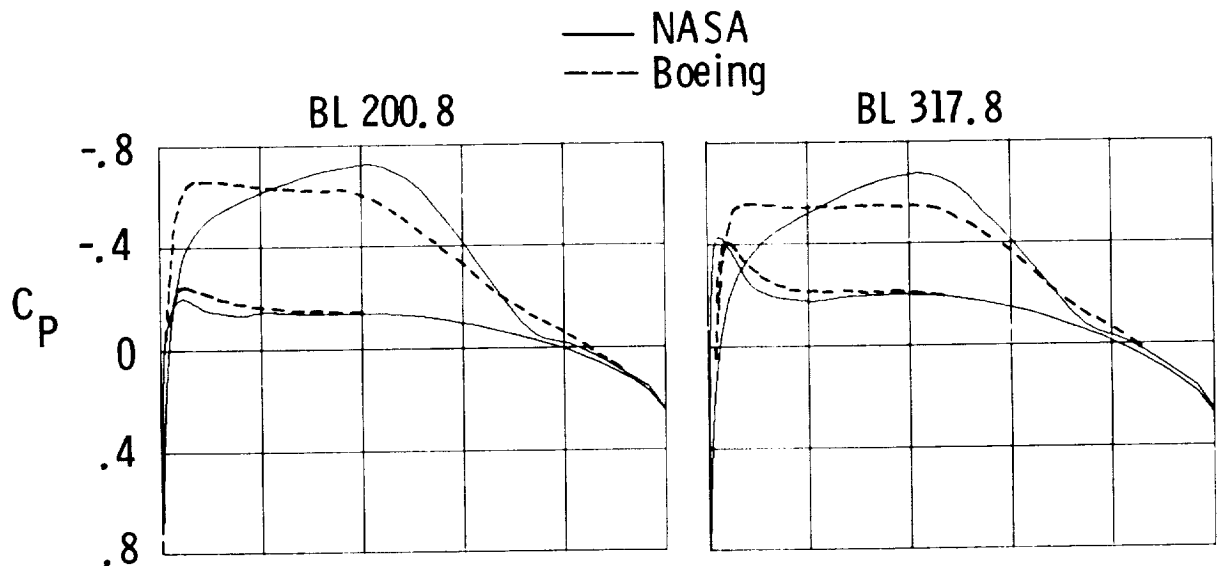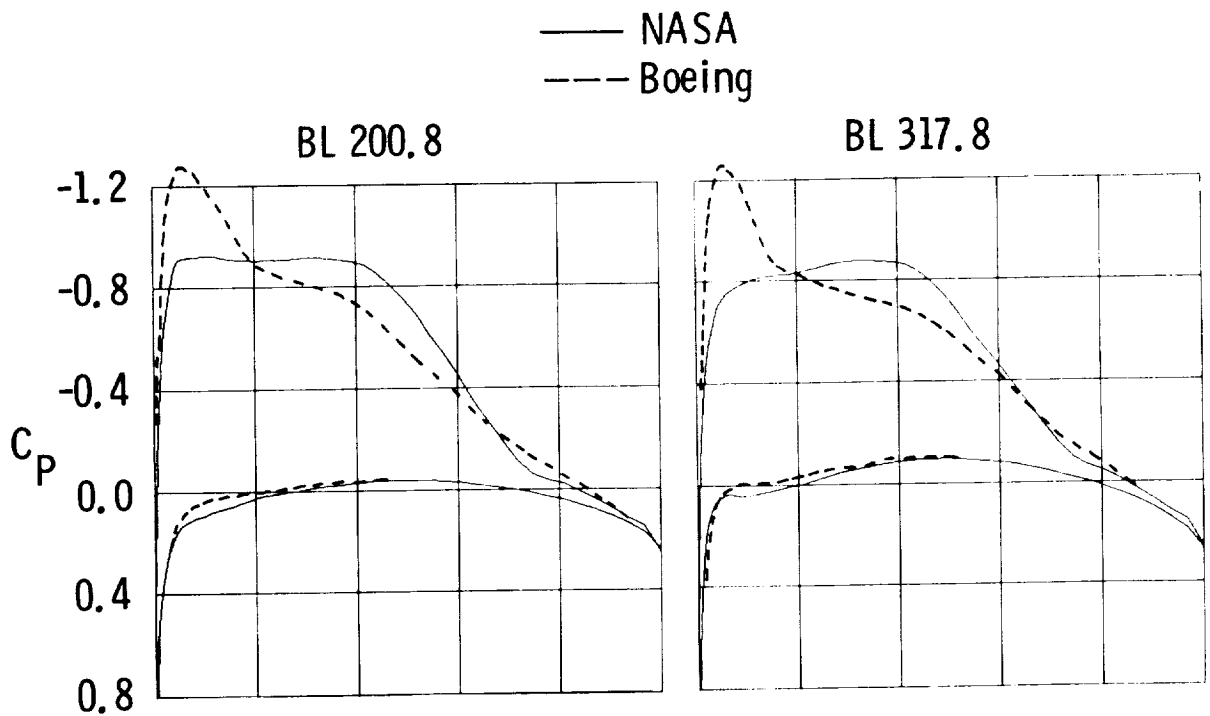
(b) M = 0.7; α = 2.95°.

Figure 11.- Three-dimensional analysis of F-14 glove design.

———— NASA
———— Boeing

(c) M = 0.8; α = 1.3°.

Figure 11.- Concluded.

ASPECT RATIO = 8.0
TAPER = 0.35

$\Lambda_{c/4}$ = 0.37
S_W = 250 FT^2

B/2 = 252.6 IN.
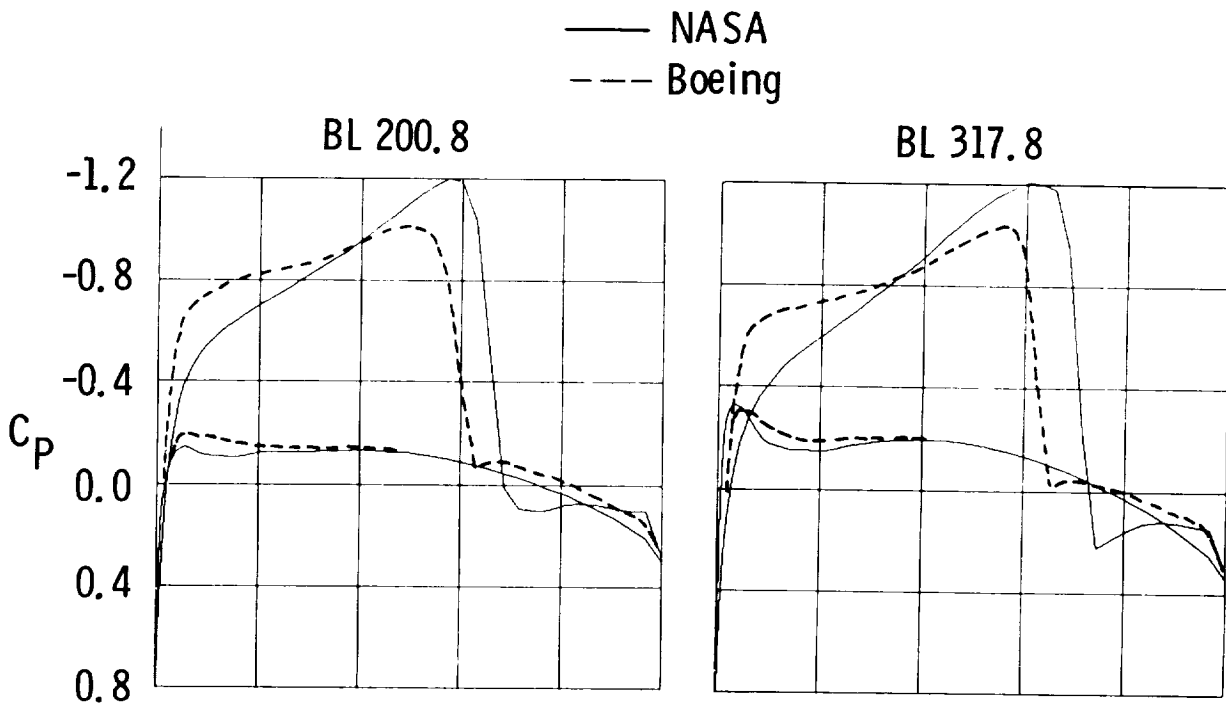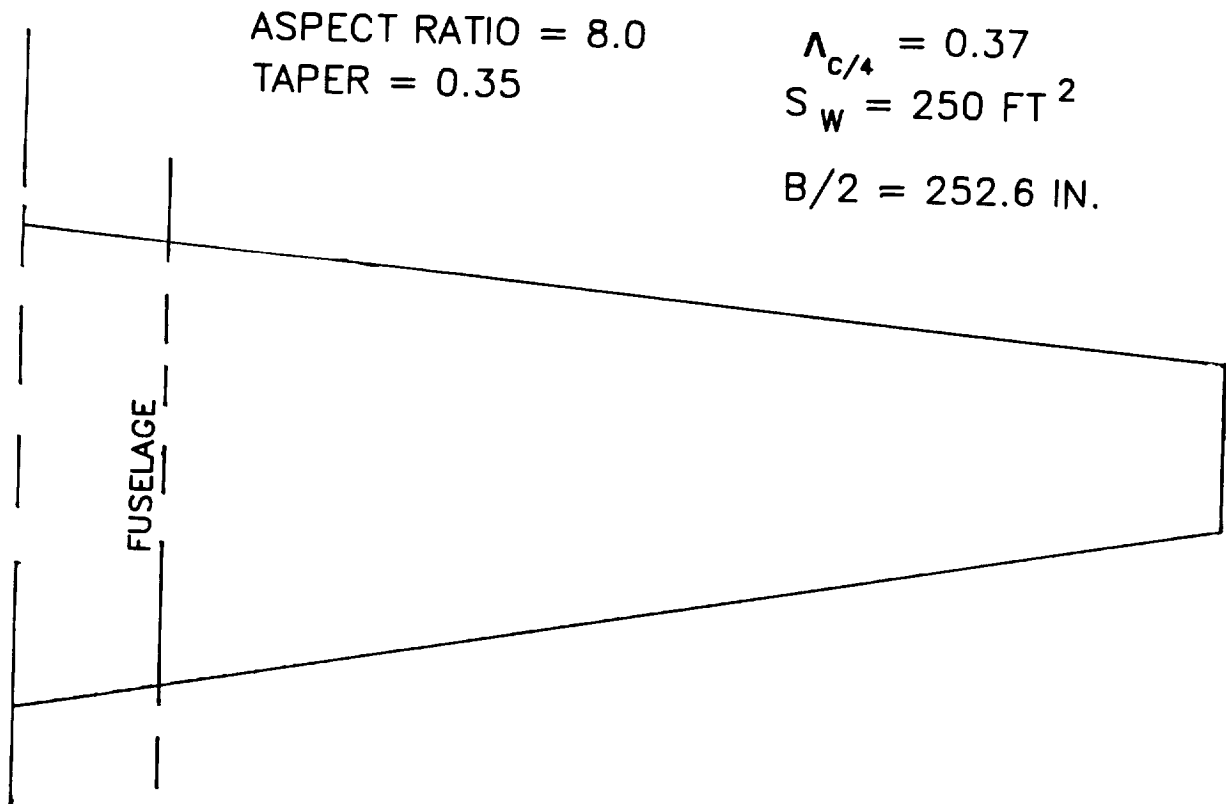
Figure 12.- High-aspect-ratio NLF wing planform.

C-2

$$M = 0.70 \quad C_l = 0.25 \quad Rn = 11 \times 10^6$$
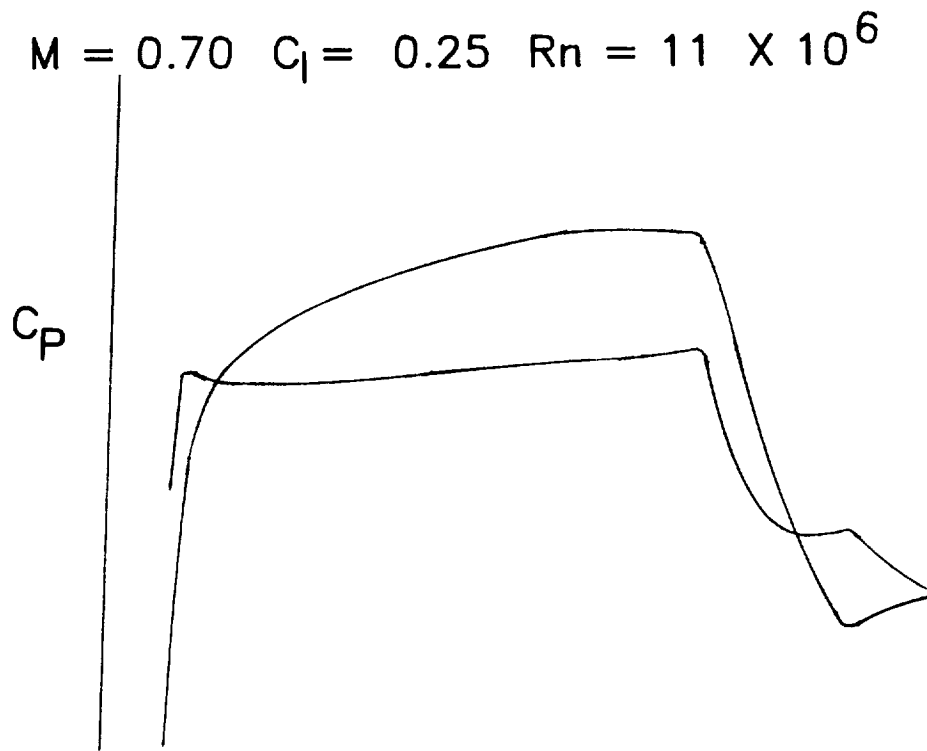
Figure 13.- Two-dimensional analysis of initial airfoil design.

$$M = 0.70 \quad C_l = 0.25 \quad Rn = 11 \times 10^6$$
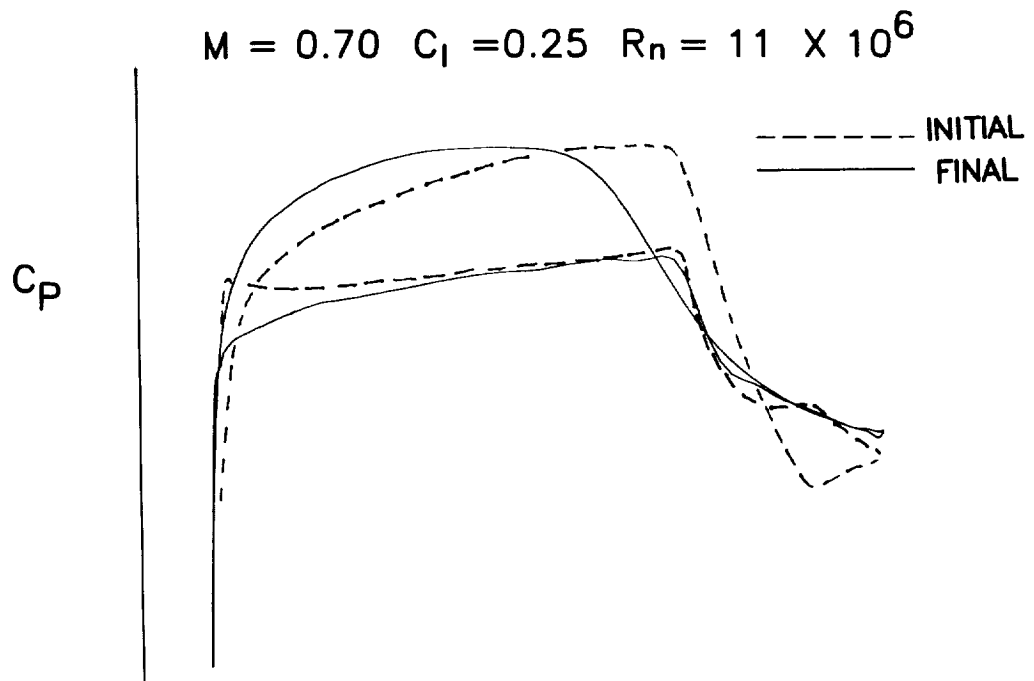
Figure 14.- Two-dimensional analysis of combination airfoil design.

86
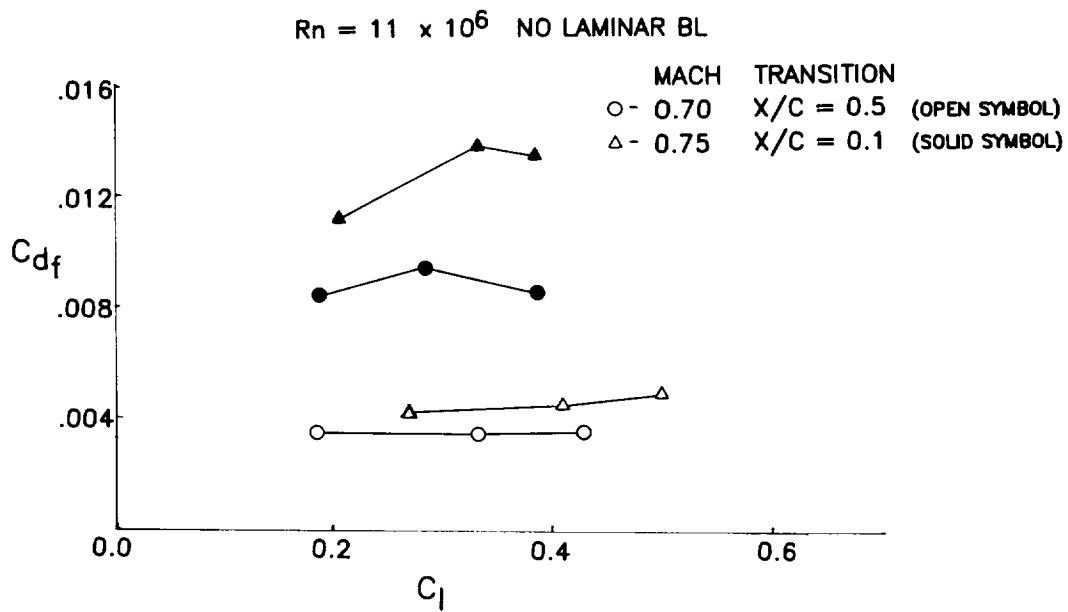
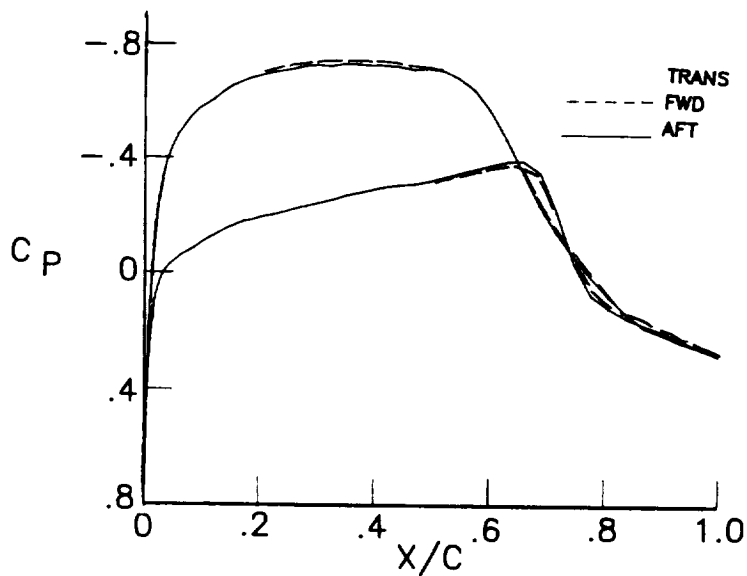Figure 15.- Variation of skin-friction drag coefficient with sectional lift coefficient.

Figure 16.- Three-dimensional analysis of final wing design.